Z. Kristallogr. Suppl. **26** (2007) 399-404

Structure properties of chemisorbed methyl groups in the framework of faujasite zeolitic catalysts

S. Vratislav[1,*], M. Dlouhá[1], V. Bosáček[2]

[1]Faculty of Nuclear Sciences and Physical Engineering CTU in Prague
[2]Heyrovský Institute of Physical Chemistry of AS ČR
[*] Contact author; e-mail: stanislav.vratislav@fjfi.cvut.cz

Keywords: neutron powder diffraction, structure analysis, zeolitic catalysts

Abstract. Zeolites and related microporous materials have common and diverse applications. Chemisorbed methyl groups in the zeolitic lattice belong to the most important problems of surface chemistry. Knowledge of structures has been quite important for developing new materials, as well as for tailoring properties of existing materials. The aim of our study was to determine regular distribution of cations and chemisorbed species over the lattice of NaX, NaLSX and NaY zeolites (i.e. to locate chemisorbed CH_3^+ or CD_3^+ ions at different oxygen atoms) by powder neutron diffraction and ^{13}C MAS NMR method. The complete structure parameters of NaX and NaLSX type of zeolitic catalysts were determined by Rietveld analysis of powder neutron patterns using the GSAS package.

Introduction

To understand the properties of zeolites it is necessary to determine the structure arrangement of these microporous compounds. Chemisorbed methyl groups in the zeolitic lattice belong to the most important problems of surface chemistry. Theoretical investigations [1] demonstrated that chemical properties of protons are controlled by actual basicity of the lattice oxygen atoms and by the character of bonds where protons are attached. It is well known that chemisorbed carbenium ions on zeolites and other alumosilicates are bonded to basic lattice oxygen atoms, forming thus surface alkoxy species [1]. Experimental support was obtained also from the results of diffraction methods, where namely neutron diffraction provided direct evidence on the location of protons in faujasites with various H+/Na+ ratio [2]. Preparation of the surface alkoxy species is based usually on the reaction of methyliodide with zeolitic cations or acid protons. Methylium ions, evolved in the reaction of adsorbed methyliodide with reactive free sodium cations (or acid protons), create the bridging form of surface methoxy compounds which are detected by ^{13}C MAS NMR with typical chemical shift of their signal [2,3]. The chemical shift of bridging methoxy carbon is very sensitive to the electronegativity of the lattice oxygen atom. It is evident that chemisorbed methylium ions (cations) take part in the charge compensation of the skeleton negative charge and that they substitute the removed plus charges of zeolitic cations (or acid protons in OH) producing e.g.

sodium iodide clusters in extra-lattice positions or water molecules as in the case of the reaction of methanol with OH groups.
The aim of our study was to estimate the regular distribution of cations and the location of chemisorbed species CH_3^+ or CD_3^+ in the lattice of the chemisorbed zeolitic catalysts (faujasite type). Further, we try to elucidate the role and participation of various lattice oxygen types in chemisorption of methyl cations.

Experiment

Well-developed crystals of NaY, NaX and NaLSX with high content of sodium cations and with low content of defects and decationation were used in our studies. Chemical composition of investigated dehydrated zeolites of NaX and NaY was

$Na_{80.0}Ca_{1.2}[(AlO_2)_{82.4}(SiO_2)_{109.6}]$ and $Na_{48.9}Ca_{1.6}[(AlO_2)_{52.1}(SiO_2)_{139.9}]$

respectively. Preparation of samples for neutron diffraction and MAS NMR experiments was

Table 1. Diffractogram information[a].

Data type	NaLSX	NaLSX + $CH_3(CD_3)$
data collection temperature /K/	7	7
space group	Fd3	Fd3
a /nm/	2.49813(5)	2.49361(6)
Profile factor R_p	0.0538	0.0573
Weighted profile factor R_{wp}	0.0427	0.0436
χ^2	2.015	2.022
Wavelength (nm)	0.13621	0.13621
Zero correction (deg)	-3.20	-3.18
Scale factor	438	416
Number of reflections	843	843
Profile function	Gauss	Gauss
Asymmetry correction	4.21	4.21
U,V,W	6 582, -4569, 316	5438, -3784, 325
background function	cosine Fourier series	cosine Fourier series

Remarks: [a]Rietveld refinement was used to minimize $\Sigma w_i (I_{o,i} - I_{c,i})^2$ where $I_{o,i}$ and $I_{c,i}$ are the observed and calculated powder diffraction intensities for the ith point, respectively. Weights w_i are $1 / I_{o,i}$. Weighted and unweighted profile R factors are defined as $R_{wp} = \{[\Sigma w_i (I_{o,i} - I_{c,i})^2] / [\Sigma w_i (I_{o,i})^2]\}^{1/2}$ and $R_p = \Sigma |I_{o,i} - I_{c,i}| / \Sigma I_{o,i}$. χ^2 was calculated from $(R_{wp} / R_e)^2$.

described in [2,3]. Powdered zeolite was then transferred under vacuum into thin-glass cylindric vessel (diameter of 12 mm, height of 35 mm) and sealed off for diffraction experiment. The portion of the same sample was sealed off under vacuum in a tube for the test controle ^{13}C MAS NMR spectra measurement on a BRUKER DSX200 spectrometer (details see in [3]). A valuable information on the conversion of methyl iodide to methoxy species was obtained by this NMR method.
Neutron powder diffraction patterns were collected at temperature of 298 K and 7 K on the KSN-2 diffractometer, which is placed at the LVR-15 research reactor in Řež near Prague [4]. This device was equipped with close circuit liquid helium cryostat - type CP-62-ST/5 (Cryophysics SA). The wavelength of 0.13621 nm was used and the resolution $\delta d/d=0.00075$ was achieved. The complete structural parameters were determined by Rietveld analysis of powder neutron diffraction data using the GSAS software package [5]. A difference Fourier maps showed the positions of chemisorbed methyl groups and distribution of cations after chemisorption. Some experimental parameters of the neutron diffractometer KSN-2 and characteristic features of the refinement processing are given in table 1.

Results and discussion

The diffraction patterns (collected at 7 K or 294 K) of chemisorbed samples were used to determine the complete set of structure parameters. The results of the structure analysis of our chemisorbed samples were published at [6-8] for NaX and for NaLSX are given in table 2. Parameters of NaLSX were refined in both recently discussed space groups [9] i.e. in the Fd3 space group and in the Fddd (orthorhombic) group but without any significant difference. Zeolite LSX (low silica X) has a Si/Al ratio of 1 and represents the highest number of charge-compensating cations of all faujasites.
Our experimental data allow to compare the changes in the occupation of positions of the lattice atoms in original evacuated NaX and in the same sample after chemisorption of methyl iodide. These changes were detected not only with occupation factors of cationic sites but sometimes also in coordinates of Na^+ cations where a splitting (at 7 K) is demonstrated of the position SI' into two sites Na2 and Na3 (see table 2), which are separated at helium temperature but merged at room temperature. Cations are distributed over six possible sites as proposed by Olson [10]in the frame of the Fd3 space group. In recent publications [11,12] the distribution of Na^+ cations in faujasites was also tested by high resolution ^{23}Na MAS NMR. The NMR results altogether confirm the results from diffraction methods. Cations in SII positions are represented after chemisorption only with the fully occupied Na4 site (32 per unit cell).
Structure parameters of methyl groups were determined by means of a difference Fourier maps, where nuclear density contours at the O1 and the O4 oxygen denoted M1 and M2 (table 2) are given in table 3. We observed fact that their distances from the oxygen atoms the M1-O1 (or M1-O4) and M2-O1 (or M2-O4) given in table 3 are spread in the interval from 0.15 to 0.17 nm. It has been shown that in NaLSX the position M1 as well as M2 assigned to CH_3-group (or CD_3-group) exhibit a shorter distance to O4 than to O1, although in NaX structure the situation is inverse. It is assumed that this effect is associated with the amount of particles in supercages. Comparing this distance with the published C-O bond length of compact nonporous crystals (for bridging methoxy group, e.g. in dimethyl-aluminium methoxide trimer 0.1436 nm [13] or in trinuclear methoxy-bridged Ti-Mg complexes d = 0.1417 nm

[14]), it is clear that the distances observed by us in microporous crystals are longer. To analyze this problem, it would be necessary to take into consideration at least two factors: firstly

Table 2. Fractional coordinatesa, occupation numbers and standard deviationsb of Na+ cations and chemisorbed methyl groups for A) NaLSX - initial and B) NaLSX with chemisorbed CD3I at 7 K..

Atom	site	P	x	y	z	U_{iso} / $Å^2$/
A) NaLSX - initial						
Na1	16c	0.11(5)	0.00000	0.00000	0.00000	-
Na2	32e	0.96(7)	0.0489(7)	0.0489(7)	0.0489(8)	0.051(7)
Na3	32e	-	0.0583	0.0583	0.0581	-
Na4	32e	0.99(5)	0.2311(2)	0.2311(2)	0.2311(4)	0.009(2)
Na5	96g	0.14(4)	0.421	0.323	0.160	-
Na6	96g	0.11(4)	0.435	0.278	0.167	-
Na6´	96g	0.12(4)	0.467	0.314	0.155	-
B) NaLSX – chemisorbed CD_3						
Na1	16c	-	0.00000	0.00000	0.00000	-
Na2	32e	0.72(6)	0.0487(7)	0.0487(7)	0.0488(8)	0.045(7)
Na3	32e	0.23(5)	0.0583	0.0583	0.0585	-
Na4	32e	1.03(4)	0.2306(2)	0.2306(2)	0.2305(4)	0.008(2)
Na5	96g	-	0.421	0.323	0.160	-
Na6	96g	-	0.435	0.278	0.167	-
Na6´	96g	-	0.467	0.314	0.155	-
Na7[c]	96g	0.32(5)	-0.209(3)	0.295(3)	0.088(3)	0.052(8)
M1[d]	96g	0.14(3)	-0.138(5)	0.192(5)	0.109(4)	0.057(9)
M2[d]	96g	0.14(3)	-0.138(5)	0.108(4)	0.192(4)	0.059(8)
I[e]	96g	0.29(3)	-0.214(5)	0.192(4)	0.192(4)	0.046(7)

[a] Origin at $\bar{3}$ of Fd3; A) a_o= 2.49813 (5) nm, B) a_o= 2.49361 (6) [b] Values in parentheses are the estimated standard deviations of the last digit. [c] Position not detected in the original evacuated NaLSX crystals. [d] M1 and M2 positions of the supposed chemisorbed methyl groups. [e] Position assigned to iodine in created NaI clusters.

Table 3. Selected distances of chemisorbed methyl groups from lattice oxygen O1 and O4.

zeolitic catalyst	T /K/	CH_3I^* 1mol/u.c	M1-O1 /nm/	M1-O4 /nm/	M2-O1/nm/	M2-O4 /nm/
NaX	7	15.3	0.1653(5)	0.1764(4)	0.1661(5)	0.1789(4)
NaLSX	7	26.4	0.1573(6)	0.1535(5)	0.1712(6)	0.1572(5)
NaLSX	298	24.8	0.1627(6)	0.1530(5)	0.1656(6)	0.1548(5)

Remarks: *Adsorbed molecules per unit cell M1, M2 – chemisorbed methyl groups

rotation and precession mobility of the C-O bond of anchored methyl group, and secondly, interactions of methyl hydrogens (or deuteriums) with other species in their vicinity, e.g. with other lattice oxygen atoms [6]. Nevertheless, the O-C distance lengthening may be also associated with the interaction of the considered chemisorbed CH_3 (or CD_3) group with other species. Further, may be take into consideration strong intermolecular interactions [13,14] or the influence of force field gradients in the zeolitic supercavities.

Concluding remarks

In consideration of our results we can conclude:
-The complete structure parameters of NaY [4], NaX [6-8] and NaLSX (see table 2) type of zeolitic catalysts in initial form and after chemisorption were determined from our powder neutron diffraction measurements. Our structure parameters of an initial dehydrated NaX and NaLSX samples at room temperature are well in line (considering various composition of materials and experimental deviations) with results (including cation distribution) of the previous studies [9,10].
-Methylium ions are located in NaX and NaLSX faujasite at O1 and O4 lattice oxygen atoms only in α-supercavity. The location at two different sites corresponds well with two observed ^{13}C MAS NMR signals at 54 and 58 ppm of surface bridging methoxyls. We have shown in the previous studies [4,6] that methyl groups are located in NaY at positions associated with oxygen atoms O1.
-Chemisorption of methylium ions at nucleophilic lattice oxygen sites has a remarkable effect on the distribution of cations in the lattice. It demonstrates that long-range forces and variations of electrostatic field gradients significantly change the cations distribution.
-Neutron powder diffraction is very valuable for this work, since single crystals are rarely available and because understanding the sitting of light atoms is paramount.

References

1. Mortier, W.J., Sauer, J., Lercher J. A., Noller, H.,1984, *J. Phys. Chem*., **88**, 905-910.
2. Jirák, Z., Vratislav, S., Bosáček, V.1980, *J. Phys. Chem. Solids*, **41**, 1098-95
3. Bosáček V., *1993, Phys. Chem.*, **97**, 10732-10735.
4. Vratislav, S., Dlouhá, M., Bosáček, V., 2000, *Physica B,* **276 - 278**, pp.926-931.
5. Von Dreele R. B., 1997, *J. Appl. Cryst.*, **30**, pp.517-520.

6. Vratislav, S., Dlouhá, M., Bosáček, V., 2002, *Applied Physics A*, **74**, 1320-21.
7. Vratislav S., Dlouhá M., Bosáček V., 2004, *Physica B*, **350,** 407-411
8. Vratislav S., Dlouhá M., Bosáček V., 2006, *Acta physica slovaca*, **56**, 137-140.
9. Czjzek M., Jobic H., Fitch A.N., Vogt T.*,*1992, *J. Phys. Chem*., **96**, 1535 -1538.
10. Olson D. H.,1995, *Zeolites*, **15**, 439-444.
11. Plevert J., Di Renzo F., Fajula F., Chiary G., 1997, *J. Phys. Chem. B*, **101**, 10340-10343.
12. Baehtz C., Fuess H., *Phys. Chem. Chem. Phys.*, 2002, **4,** 4543-4548.
13. Gyepes R., Hiller J., Thewalt U., Polášek M., Šindelář P., Mach K., 1996, *J. Organomet. Chem.*, **516***,* 177-182.
14. Blaszkowski S.R., van Santen R.A., 1995, *J. Phys. Chem.*, **99**, 1728-1733.

Acknowledgements. This research has been supported by MŠMT grant No. MSM 6840770021 and by GA CAS CR grant No. IAA100100611.

Z. Kristallogr. Suppl. **26** (2007) 405-410

Pressure-induced over-hydration in scolecite: A synchrotron powder diffraction study

A.Yu. Likhacheva[1], Yu.V. Seryotkin[1], A.Yu. Manakov[2], S.V. Goryainov[1], A.I. Ancharov[3], M.A. Sheromov[4]

[1] Institute of Geology and Mineralogy SibD RAS, Novosibirsk
[2] Institute of Inorganic Chemistry SibD RAS, Novosibirsk
[3] Institute of Solid State Chemistry SibD, Novosibirsk
[4] Budker Institute of Nuclear Physics SibD RAS, Novosibirsk
[*] Contact author; A.Yu. Likhacheva; e-mail: alih@uiggm.nsc.ru

Keywords: zeolite, scolecite, high pressure, over-hydration, compressibility

Abstract. The compressibility of the natural fibrous zeolite scolecite in aqueous medium was studied using *in situ* synchrotron powder diffraction data collected using a diamond anvil cell (DAC). At 1 GPa the regular compression of the lattice is interrupted, suggesting the onset of over-hydration. At 1.23 GPa scolecite undergoes a transformation to a high-hydrated phase, which is expanded by 5.0 % due to the increase of the water content in the channels. According to the proposed structural model, the symmetry of the high-pressure phase is reduced to *C*1. The evolution of lattice parameters of scolecite up to 4.4 GPa is discussed in terms of the framework deformation influenced by the penetration of additional water molecules.

Introduction

Fibrous narrow-pore zeolites, owing to the high flexibility of their frameworks, exhibit anomalous volume expansion upon compression in aqueous medium due to the penetration of additional water molecules into the framework channels [1,2]. A detailed structural study of the Na-member of this group (natrolite) revealed two additional water positions in the channels of the high-hydrated phase and an associated 4.2% volume expansion [1-3]. The framework channels of scolecite $Ca[Al_2Si_3O_{10}] \times 3H_2O$ accommodate one cation (Ca) and three water molecule sites (O6, O60, O7 [4]). The different water-cation arrangement in scolecite ($Ca+3H_2O$) with respect to that of the isomorphic natrolite ($2Na+2H_2O$) would imply a different mechanism for the pressure-induced over-hydration. In this work the evolution of the lattice parameters of scolecite compressed in water medium to 4.4 Gpa is characterized in connection with the refined structure of low-pressure (LP) phase near the transition point, as well as the structure model proposed for the high-pressure (HP) phase. This allows us to describe some general features of the deformation mechanism in scolecite during the over-hydration.

Experimental

We used finely ground sample of scolecite (Berufjord, Iceland), with chemical formula: $Ca_{0.97}Na_{0.02}[Al_{1.96}Fe_{0.02}Si_{3.02}O_{10}]\times 3.04H_2O$ (by X-ray fluorescence analysis). The cell parameters at ambient conditions are a = 18.5054(9), b = 18.9776(11), c = 6.5276(4) Å, β = 90.588(5)°, V = 2292.30(16) Å^3 (space group $F1d1$). The powder diffraction experiments were performed to 4.4 GPa at the 4th beamline of the VEPP-3 storage ring of the Synchrotron Centre SSRC, Novosibirsk, at a fixed wavelength of 0.3675 Å, using a DAC and methanol-ethanol-water (4:1:1) as the pressure-transmitting medium. A MAR345 imaging plate detector (pixel dimension 100 μm) was used.

Rietveld refinements of the lattice and atomic parameters (at 1.06 and 1.6 GPa, figure 1, table 1) were performed using the GSAS set of programs in the 2Θ range 3-20°. The Si-O and Al-O distances were restrained to 1.62(2) Å and 1.74(2) Å, the refined mean values

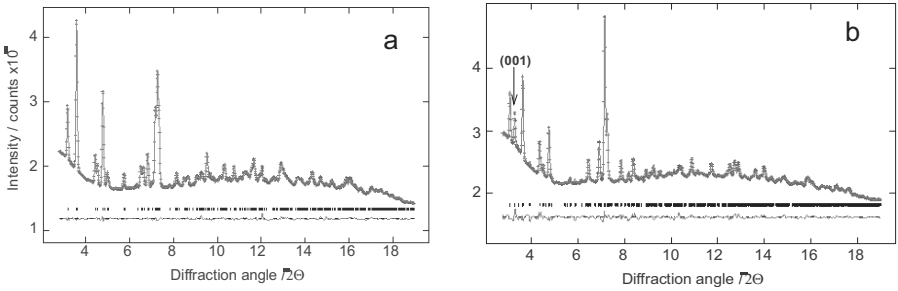

Figure 1. Results of Rietveld refinements at 1.06 GPa (a, LP structure) and 1.6 GPa (b, HP structure).

being of 1.627(9) and 1.740(9) Å for the LP phase and 1.62(1), 1.73(1) Å for the HP phase, respectively. The crystal structure of natural scolecite [4] was used as a starting model for the

Table 1. Selected crystallographic and experimental data for scolecite at high pressures.

Pressure (GPa)	**1.06**	**1.6**
a (Å)	18.508(1)	19.341(6)
b (Å)	18.926(1)	19.300(6)
c (Å)	6.5120(3)	6.4101(5)
α (°)	90	90.32(2)
β (°)	90.567(5)	90.31(3)
γ (°)	90	90.08(2)
V (Å^3)	2281.0(1)	2392.8(4)
Space group	$F1d1$	$C1$
Radiation	X-ray synchrotron λ = 0.3675 Å	
2Θ range (°)	3-21	3-20
Number of observations	1849	1831
Number of variables	60	198
Number of reflections	801	3759
R_p , R_{wp}	0.0048, 0.0065	0.0058, 0.0082
R_{F2}	0.12	0.14
χ^2	0.29	0.50

refinement of the LP structure at 1.06 GPa (figures 1a, 2, table 2). Difference Fourier synthesis revealed a strong density maximum ascribed to an additional extra-framework H_2O site with small occupancy, which was introduced into the HP structure model as a 4th H_2O position (figure 2). For the HP phase, the *C*1 space group was assumed, based on the assignment of the intense peak at 3.27^o 2θ in the HP phase pattern to the (001) reflection (figure 1b). The intensity of this peak was found to strongly depend on the water-cation arrangement in the channels; in particular, it increased appreciably when half of the Ca+4H_2O groups were moved to alternative pseudo-symmetric positions relative to the LP structure (figure 2). But the strongest growth on the (001) peak was observed with the introduction of a 5th H_2O position which was supposed to lie close to the vacant cation position in the centre of the channel. Subsequent Rietveld refinement confirmed a full occupancy for this position. The resulting HP structure of scolecite (figure 2) presents a reasonably realistic, partially refined structure model that fits the experimental data; it seems to reflect some essential features of the high-hydrated scolecite and worthwhile to be shortly described in this paper.

Results and discussion

As compared to the ambient pressure, at 1.06 GPa the scolecite structure does not change appreciably, except for a strong density maximum (≈ 2 e/Å^3) revealed by the difference Fourier synthesis (figure 2, table 2). Due to its low refined occupancy (≈ 0.1), this maximum may be considered as a defect extra-framework H_2O site, indicating the over-hydrated state of the scolecite structure (a precursor of the high-hydrated phase).

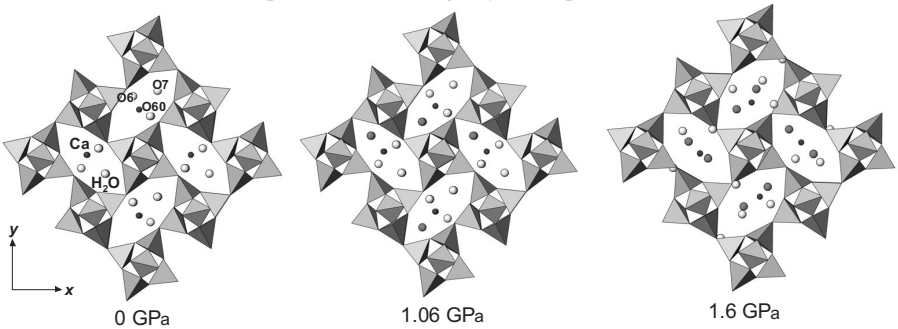

Figure 2. Crystal structure of scolecite at ambient pressure, by [4], 1.06 GPa and 1.6 GPa (structure model). The framework (Si,Al)-O_4 groups are drawn as tetrahedra, the new H_2O sites at 1.6 GPa and additional electron density at 1.06 GPa are filled dark to underline the evolution of over-hydration.

The model of the HP structure refined at 1.6 GPa is shown in figure 2 (the atomic coordinates are omitted due to restricted length of the paper). As compared to the LP structure at 1.06 GPa, the unit cell volume increases by 5.0 % due to the rotation of $[T_2O_5]^{\infty}$ chains about the common O atoms: mean T-O-T angle between the chains increases from 135^o to 146^o. This results in an expansion of the channels and a drastic increase of *a* and *b* cell parameters by 4.4 and 1.7 %, respectively, and a compensative decrease of *c* parameter by 1.8 %. The observed expansion is caused by the appearance of two additional H_2O positions in the channels, one of them being close to the position where additional electron density was found in

the LP structure. The refined occupancy for both positions is close to 1, whereas some of the ring positions (O6,O60 [4]) have lower occupancies of about 0.5.
Additional hydration of scolecite produces a fundamental reorganization of the ionic-molecular ensemble. The ($4O_{framework}$+$3H_2O$) calcium coordination in the LP structure is replaced by the ($3O_{framework}$+$4H_2O$) coordination in the HP structure model. Half of the Ca+$4H_2O$ groups are rotated by 180° and shifted by 1/2 of **c** axis. Due to the expansion of framework channels, the mean Ca-$O_{framework}$ and Ca-H_2O distances increase from 2.51 and 2.4 Å in the LP structure to 2.7 and 2.5 Å in the HP structure, respectively. The implantation of the additional H_2O positions into the HP structure channels produces several short (< 3 Å) H_2O-H_2O distances, which implies the formation of a complex network of hydrogen bonds in

Table 2. Positional parameters for scolecite at 1.06 GPa.

Atom	Occupancy	*x/a*	*y/b*	*z/c*
Si1	1.0	0.0	-0.1195(6)	0.0
Si2	1.0	0.1479(7)	0.0827(5)	0.6225(19)
Si20	1.0	-0.1624(9)	-0.3368(5)	0.6204(19)
Al1	1.0	0.0315(8)	-0.0312(6)	0.6037(19)
Al10	1.0	-0.0482(8)	-0.2144(6)	0.6129(20)
O1	1.0	0.0148(11)	-0.0485(8)	0.8680(22)
O10	1.0	-0.0170(10)	-0.1882(8)	0.8583(23)
O2	1.0	0.0674(8)	0.0531(7)	0.5854(31)
O20	1.0	-0.0846(9)	-0.2983(7)	0.6454(29)
O3	1.0	0.0892(11)	-0.0963(7)	0.5231(28)
O30	1.0	-0.1073(10)	-0.1476(7)	0.5329(28)
O4	1.0	0.1985(9)	0.0217(8)	0.7215(29)
O40	1.0	-0.2268(10)	-0.2836(8)	0.6835(27)
O5	1.0	0.1836(7)	0.1096(10)	0.4082(24)
O50	1.0	-0.1778(6)	-0.3640(9)	0.3864(23)
O6	1.0	0.0317(11)	0.0727(10)	0.0692(34)
O60	1.0	-0.0540(12)	-0.3333(10)	0.1668(30)
O7	1.0	0.0633(11)	0.2065(9)	0.3634(32)
Ca	1.0	0.2240(7)	-0.1095(5)	0.6033(22)
O70*	0.1	-0.092	0.033	0.98

*the position of strong density maximum in the difference Fourier map

which each water molecule is bonded to at least one nearest H_2O molecule. Analysis of the positional relationship of all the non-framework atoms shows that such a structure seems to be realistic enough: the H_2O-H_2O and H_2O-$O_{framework}$ distances vary between 2.6-3.0 and 2.5-3.0 Å, respectively, whereas the angles ∠ H_2O-H_2O-H_2O range from 95° to 145°. Due to the low "reflections-to-refined parameters" ratio for the triclinic HP structure model we could not refine all the H_2O-H_2O distances, some of which were fixed at 2.6 Å. We consider the present model as a base for a more constrained model involving rigid bodies in the framework part of the structure, which we plan to apply in further structure refinement.

Evolution of the unit cell parameters at high pressure

In the pressure range between 0.0001-0.9 GPa the reduction of lattice parameters is almost linear and isotropic (figure 3, table 3) in contrast to compression in a non-penetrating medium, where the direction **c** is less compressible than the directions **a** and **b** (directions **b** and **c** in the *Cc* group used in [5]). Such an isotropic compression may be considered as an

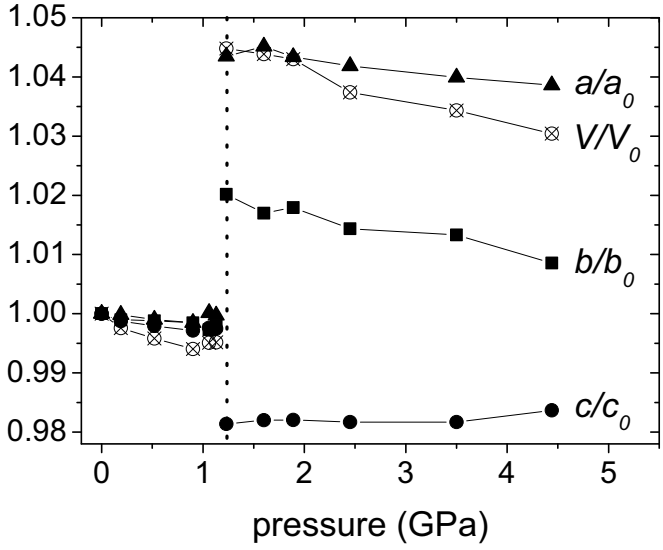

Figure 3. Unit cell parameters of scolecite, normalized to room conditions values, vs. *pressure. Estimated standard deviations are within the symbols.*

indirect evidence that the accumulation of minor defect H_2O positions starts at very low pressure, preventing the preferred contraction of the lattice along the directions **a** and **b**. The regular decrease of parameters is interrupted at 1 GPa, demonstrating an early over-hydration of scolecite. This agrees with the Fourier difference synthesis which reveals the presence of a strong density maximum at 1.06 GPa interpreted as a defect H_2O site (figure 2). The transition to the high-hydrated phase at 1.23 GPa is accompanied by the volume expansion by 5.0 % due to the increase of the zeolitic water content from 3 to 4.6 molecules per formula unit, according to our preliminary HP structure model. The main deformation mechanism here is the cooperative rotation of $[T_2O_5]^{\infty}$ chains which is the reverse of the structure compression observed in non-penetrating medium ([5]): it leads to the enlargement of the cross-section of the main channels parallel to **c** and the corresponding decrease of the ψ angle of mutual rotation of the framework chains ([6]) from 20.8° to 16.5°.

As can be seen in figure 3, the parameter *a* is slightly more sensitive to the penetration of additional water molecules into the structure channels. This results in the appearance of a pseudo-tetragonal lattice with similar parameters *a* and *b* for the HP phase at 1.23 GPa (table 3). At 1.2-4.4 GPa the contraction of the HP structure proceeds at the expense of *a* and *b* parameters, whereas parameter *c* retains its value. This behavior is similar to that of super-hydrated natrolite [1] and agrees with the model of [7] on the elastic behavior of fibrous zeolites: the tetragonal topological symmetry strongly controls the structural deformation

mechanism, when the structure deformation is no longer influenced by the penetration of additional water molecules.

Table 3. Lattice parameters and volumes of scolecite at different pressures.

P **(GPa)**	***a*** **(Å)**	***b*** **(Å)**	***c*** **(Å)**	***α*** **(°)**	***β*** **(°)**	***γ*** **(°)**	***V*** **(Å^3)**
Space group *F*1*d*1							
0	18.5054(9)	18.9776(11)	6.5276(4)	90	90.588(5)	90	2292.3(2)
0.19	18.502(2)	18.958(1)	6.5194(4)	90	90.57(1)	90	2286.7(2)
0.52	18.487(2)	18.955(2)	6.514(1)	90	90.57(1)	90	2282.7(3)
0.9	18.477(2)	18.948(2)	6.509(1)	90	90.62(1)	90	2278.6(2)
1.06	18.508(1)	18.926(1)	6.5120(3)	90	90.567(5)	90	2281.0(1)
1.13	18.500(5)	18.939(4)	6.511(1)	90	90.58(3)	90	2281.2(5)
Space group *C* 1							
1.23	19.31(1)	19.36(1)	6.406(1)	90.20(5)	90.37(2)	90.04(4)	2395(1)
1.6	19.341(6)	19.300(6)	6.4101(5)	90.32(2)	90.31(3)	90.08(2)	2392.8(4)
1.89	19.308(6)	19.318(5)	6.4104(4)	90.35(2)	90.33(2)	90.08(2)	2390.9(4)
2.45	19.28(2)	19.25(2)	6.408(1)	90.56(4)	90.39(7)	90.27(5)	2378(1)
3.5	19.244(14)	19.23(1)	6.408(1)	90.41(3)	90.3(1)	90.15(4)	2371(1)
4.44	19.22(2)	19.14(2)	6.421(1)	90.61(4)	90.2(1)	90.06(8)	2362(2)

References

1. Lee, Y., Vogt, T., Hriljac, J.A., Parise, J.B., Artioli, G., 2002, *J. Amer. Chem. Soc.*, **124**, 5466.
2. Seryotkin, Yu.V., Bakakin, V.V., Fursenko, B.A., Belitsky, I.A., Joswig, W., Radaelli, P.G., 2005, *Eur. J. Mineral.*, **17**, 305.
3. Colligan, M., Lee, Y., Vogt, T., Celestian, A.J., Parise, J.B., Marshall, W.G., Hriljac, J.A., 2005, *J. Phys. Chem. B*, **109**, 18223.
4. Joswig, W., Bartl, H., Fuess, H., 1984, *Z. Kristallogr.*, **166**, 219.
5. Comodi, P., Gatta, G.D., Zanazzi, P.E., 2002, *Eur. J. Mineral.*, **14**, 567.
6. Baur, W.H., Kassner, D., Kim, Ch.-H., Sieber, N.H.W., 1990, *Eur. J. Mineral.*, **2**, 761.
7. Gatta, G.D., 2005, *Eur. J. Mineral.*, **17**, 411.

Acknowledgements. We thank anonymous reviewers for their valuable remarks. This work is supported by RFBR grants 05-05-64657, 06-05-64542, SibD RAS Integration project 43 and RAS Program P-9-3.